

Discovery of Novel Human and Animal Cells Infected by the Severe Acute Respiratory Syndrome Coronavirus by Replication-Specific Multiplex Reverse Transcription-PCR

Laura Gillim-Ross,¹ Jill Taylor,¹ David R. Scholl,² Jared Ridenour,² Paul S. Masters,^{1,3} and David E. Wentworth^{1,3*}

Wadsworth Center, New York State Department of Health,¹ and Department of Biomedical Sciences, State University of New York,³ Albany, New York 12202, and Diagnostic Hybrids, Inc., Athens, Ohio 45701²

Received 20 November 2003/Returned for modification 27 January 2004/Accepted 4 April 2004

The severe acute respiratory syndrome coronavirus (SARS-CoV) is the causative agent of the recent outbreak of severe acute respiratory syndrome. VeroE6 cells, fetal rhesus monkey kidney cells, and human peripheral blood mononuclear cells were the only cells known to be susceptible to SARS-CoV. We developed a multiplex reverse transcription-PCR assay to analyze the susceptibility of cells derived from a variety of tissues and species to SARS-CoV. Additionally, productive infection was determined by titration of cellular supernatants. Cells derived from three species of monkey were susceptible to SARS-CoV. However, the levels of SARS-CoV produced differed by 4 log₁₀. Mink lung epithelial cells (Mv1Lu) and R-Mix, a mixed monolayer of human lung-derived cells (A549) and mink lung-derived cells (Mv1Lu), are used by diagnostic laboratories to detect respiratory viruses (e.g., influenza virus); they were also infected with SARS-CoV, indicating that the practices of diagnostic laboratories should be examined to ensure appropriate biosafety precautions. Mv1Lu cells produce little SARS-CoV compared to that produced by VeroE6 cells, which indicates that they are a safer alternative for SARS-CoV diagnostics. Evaluation of cells permissive to other coronaviruses indicated that these cell types are not infected by SARS-CoV, providing additional evidence that SARS-CoV binds an alternative receptor. Analysis of human cells derived from lung, kidney, liver, and intestine led to the discovery that human cell lines were productively infected by SARS-CoV. This study identifies new cell lines that may be used for SARS-CoV diagnostics and/or basic research. Our data and other *in vivo* studies indicate that SARS-CoV has a wide host range, suggesting that the cellular receptor(s) utilized by SARS-CoV is highly conserved and is expressed by a variety of tissues.

An outbreak of severe acute respiratory syndrome (SARS) occurred in Guangdong Province, People's Republic of China, in November 2002 (39). From China, SARS spread to 30 other countries and as of September 23, 2003, this outbreak had resulted in 8,098 reported cases, of which 774 were fatal (http://www.who.int/csr/sars/country/table2003_09_23/en/). Through the coordinated efforts of laboratories around the world, a novel coronavirus (CoV), designated SARS-coronavirus (SARS-CoV), was identified as the causative agent of SARS (6, 9, 14, 24, 25). This discovery was quickly followed by the publication of the complete genomic sequences of two SARS-CoV isolates and identification of specific subgenomic RNAs (sgRNAs) and proteins involved in replication (19, 28, 33). The origin of SARS-CoV has not been determined, but evidence strongly suggests that its emergence may be the result of zoonotic transmission(s) (10).

CoVs (order Nidovirales, family *Coronaviridae*) are diverse, enveloped, positive-stranded RNA viruses that produce a nested set of sgRNA molecules during replication (11, 16). CoVs are placed into group 1, 2, or 3 based on antigenic and genetic criteria (11, 16). The genome of SARS-CoV has considerable nucleotide divergence from that of other known human CoVs (HCoVs) (14, 19, 28). However, phylogenetic anal-

ysis of the SARS-CoV replicase gene demonstrated that, despite a number of unique features, SARS-CoV is most closely related to group 2 CoVs (32). Group 2 includes mouse hepatitis virus (MHV), bovine coronavirus, and HCoV-OC43. The CoV genome, approximately 27 to 32 kb in length, is the largest found in any of the RNA viruses. Large spike (S) glycoproteins protrude from the virus particle, giving CoVs a distinctive corona-like appearance when visualized by electron microscopy. The S protein is the major viral-attachment protein, critical to virus binding and fusion of the viral envelope with cellular membranes. CoVs infect a wide variety of species, including dogs, cats, pigs, mice, cows, birds, and humans (11, 16). However, the natural host range of each CoV strain is narrow, typically consisting of a single species (11, 16).

CoVs enter cells by receptor-mediated endocytosis or by fusion with the plasma membrane (11, 16). The S protein-receptor interaction is a major determinant of species specificity and tissue tropism for both group 1 and group 2 CoVs. This finding is best illustrated by the fact that CoV genomic RNA (gRNA) is infectious when transfected into nonpermissive cells and that transfection of nonpermissive cells with constructs expressing CoV receptors renders them susceptible to infection (4, 8, 11, 13, 16, 36). The receptor for group 1 CoVs, including HCoV-229E, feline CoVs, and porcine CoVs, is aminopeptidase N (APN) (4, 34, 38). Although APN is highly conserved, it is generally used in a species-specific manner (13, 35). CEACAM1a, the best-characterized CoV recep-

* Corresponding author. Mailing address: Wadsworth Center, NYSDOH, 120 New Scotland Ave., Albany, NY 12208. Phone: (518) 408-2396. Fax: (518) 473-1326. E-mail: dwentwor@wadsworth.org.

tor and a principal determinant of the tissue tropism and restricted host range of MHV (3, 7, 8, 30), is utilized by different strains of MHV, which is a group 2 CoV (11).

SARS-CoV was first isolated in African green monkey kidney (VeroE6) cells and fetal rhesus monkey kidney (FRhMK) cells inoculated with clinical specimens (6, 14, 24, 26). Based on cytopathic effect (CPE), other cells routinely used for identification of respiratory pathogens (MDCK, A549, NCI-H292, HeLa, LLC-MK2, Hut-292, B95-8, MRC-5, RDE, and Hep-2) were determined to be nonpermissive to SARS-CoV infection (6, 14, 24). Additionally, human peripheral blood mononuclear cells (PBMCs) were shown by reverse transcriptase PCR (RT-PCR) to support SARS-CoV replication (17). To determine the *in vitro* host range, analyze potential receptors, and identify additional human cell lines permissive to SARS-CoV, a multiplex RT-PCR assay for the detection of SARS-CoV replication was developed. Cells routinely used by clinical diagnostic laboratories for pathogen screening were specifically analyzed to determine their susceptibility to SARS-CoV. Additionally, primary cells and continuous cell lines derived from a number of species and tissues were analyzed for their susceptibilities to SARS-CoV. This study identified novel human and animal cells that support SARS-CoV replication.

MATERIALS AND METHODS

Propagation and titration of virus. A seed stock of SARS-CoV (strain Urbani) that was passaged twice in VeroE6 cells was kindly provided by W. Bellini and T. Ksiazek of the Centers for Disease Control and Prevention, Atlanta, Ga. This virus was amplified by two passages in VeroE6 cells to establish a high-titer stock (passage 4) that was utilized in all experiments. The 50% tissue culture infectious dose (TCID₅₀) per ml was determined for SARS-CoV in VeroE6 cells by the observation of CPE as previously described (35). Briefly, cells were plated in 96-well plates (Falcon; Becton Dickinson) at a density of 5×10^4 cells/well in 150 μ l of medium. The virus was serially diluted by half logs from 10^0 to 10^{-8} in culture medium. One hundred microliters of each dilution was added per well, and the cells were incubated 3 to 4 days at 37°C.

Biosafety containment. All experiments with infectious SARS-CoV were performed in a Biosafety Level 3 laboratory and were conducted under appropriate conditions, using precautions that adhered to or exceeded the requirements set forth by the Centers for Disease Control and Prevention Interim Laboratory Biosafety Guidelines for Handling and Processing Specimens Associated with SARS. Procedures performed with SARS-CoV included viral propagation, storage of stocks, inoculation of various cell lines, and RNA extraction.

Cell lines. The following cell lines were obtained from the American Type Culture Collection, Rockville, Md.: VeroE6, MRC-5, BHK-21, MDCK, HRT-18 (HCT-18), Mv1Lu, CMT-93, AK-D, and A549. R-Mix (R-Mix FreshCells, DHI number 96-T025; Diagnostic Hybrids, Inc., Athens, Ohio) is a mixed monolayer of mink lung cells (strain Mv1Lu) and human adenocarcinoma cells (strain A549). HEK-293T cells were kindly provided by Yoshihiro Kawaoka (University of Wisconsin, Madison). Huh-7 cells were kindly provided by Aleem Siddiqui (University of Colorado Health Sciences Center, Denver). BHK-21 and CMT-93 cells were transfected with a human APN (hAPN) expression plasmid described previously (35). pRhMK and pCMK cells were derived from adult U.S.-bred animals (DHI numbers 49-T025 and 47-T025, respectively). HEL cells were obtained from the Wadsworth Center Tissue Culture Facility. Chicken embryo fibroblast (CEF) cells were obtained from Charles River Laboratories, Inc. (Wilmington, Mass.). Unless stated otherwise, all cell lines were maintained in base medium supplemented with 10% fetal bovine serum (FBS) (HyClone, Logan, Utah), 200 U of penicillin G/ml, 200 μ g of streptomycin sulfate/ml, and 0.5 μ g of amphotericin B (Invitrogen Corp)/ml. VeroE6, HEK-293T, L2, AK-D, A549, FCWF, pCMK, pRhMK, and CMT-93 cells were maintained in Dulbecco's modified Eagle medium (DMEM). MDCK cells were maintained in DMEM supplemented with 5% FBS. HEL, Mv1Lu, R-Mix, and CEF cells were maintained in modified Eagle's medium (MEM). HRT-18 cells were maintained in RPMI 1640 (Invitrogen Corp.) supplemented with 10% horse serum (HyClone) and 1 mM sodium pyruvate (Invitrogen Corp.). Huh-7 cells were maintained in DMEM supplemented with 20% FBS. MRC-5 cells were maintained in MEM

supplemented with 1 mM sodium pyruvate and 0.1 mM MEM nonessential amino acids (Invitrogen Corp.) BHK-21 cells were maintained in DMEM supplemented with tryptose phosphate broth (1.48g/liter) (Invitrogen Corp.).

Inoculation of cells and RNA isolation. Cells seeded at a density of 2×10^6 in T25 flasks (Falcon; Becton Dickinson) 1 day prior to the experiment were inoculated with the virus at a multiplicity of infection (MOI) of ~ 0.001 in a final volume of 1 ml or were mock inoculated and incubated 1 h at 37°C. The virus was removed (1 h), and 5 ml of fresh medium was added to each flask. The cells were maintained at 37°C throughout the experiment. At 1, 24, or 48 h postinoculation, the cells were observed for CPE, the supernatants were collected for subsequent titration, and total RNA was extracted by using TRIZOL reagent (Invitrogen Corp.) and quantitated by spectrophotometer (Eppendorf). Mock inoculations were collected at 48 h postinoculation.

Multiplex RT-PCR analysis of SARS-CoV replication. Glyceraldehyde 3-phosphate dehydrogenase (G3PDH), and SARS-CoV gRNA and sRNA were detected by using multiplex one-step RT-PCR. Five oligonucleotide primers were used to simultaneously amplify three different targets. G3PDH was amplified with G3P-279 (5'-CATCACCATCTCCAGGAGC-3'), a sense primer that corresponds to human G3PDH from base 279 to base 299, and G3P-1069R (5'-CTTACTCCTTGGAGGCCATG-3'), an antisense primer that is complementary to human bases 1049 to 1069. gRNA was specifically amplified with SARS-21,263 (5'-TGCTAACTACATTTTCTGGAGG-3'), a sense primer that corresponds to bases 21,263 to 21,284 of SARS-CoV Urbani, and SARS-21,593R (5'-AGTATGTTGAGTGTAATTAGGAG-3'), an antisense primer complementary to bases 21,571 to 21,593 of SARS-CoV Urbani (28). sRNA was specifically amplified by using SARS-1 (5'-ATATTAGGTTTTTACCTACCCAGG-3'), a sense primer corresponding to bases 1 to 24 of SARS-CoV Urbani and SARS-21,593R. Amplification was carried out by using the QIAGEN OneStep RT-PCR kit. Briefly, each reaction consisted of 2 μ g of total RNA template–400 μ M (each) dNTP–200 nM (each) G3PDH primer–400 nM SARS-1–400 nM SARS-21,263–600 nM SARS-21,593R–2 μ l QIAGEN enzyme mix in a final volume of 25 μ l. The cycling parameters were 50°C for 30 min, 95°C for 15 min, 35 cycles of 94°C for 30 s, 57 to 58°C for 30 s, and 72°C for 1 min, followed by 10 min at 72°C in an Eppendorf Mastercycler gradient. To eliminate nonspecific products amplified in some cell lines, different cycling parameters were used for samples from HEL, R-Mix, A549, MRC-5, MDCK, AK-D, and HRT cells. Briefly, the touchdown parameters were 50°C for 30 min, 95°C for 15 min, 10 cycles of 94°C for 30 s, 62.3°C for 30s (–0.3°C/cycle), 72°C for 1 min, 24 cycles of 94°C for 30 s, 59.3°C for 30 s, and 72°C for 1 min, followed by 10 min at 72°C. Amplification products were analyzed by electrophoresis through a 1.5% agarose gel and visualized by ethidium bromide staining. Primers were synthesized by the Wadsworth Center Molecular Genetics Core or Invitrogen Corp.

Flow cytometry. Expression levels of hAPN were determined by fluorescence-activated cell sorter (FACS) analysis as described previously (35). DW-1, a monoclonal antibody that recognizes hAPN in the conformation recognized by the HCoV-229E S glycoprotein, was utilized. Phycoerythrin-conjugated goat F(ab')₂ anti-mouse immunoglobulin (DAKO) was used for detection. Mouse immunoglobulin G2 antibody was included as an isotype control (Pharmingen; Becton Dickinson, Franklin Lakes, N.J.). The cells were analyzed by a FACS-Calibur flow cytometer (Becton Dickinson), and data were analyzed using FlowJo software (Tree Star, Inc., San Carlos, Calif.).

RESULTS

Detection of virus entry and replication initiation. To identify an early step in the initiation of SARS-CoV infection, a novel multiplex RT-PCR assay for the detection of SARS-CoV replication was developed. This assay takes advantage of the fact that 3' coterminal sRNAs, which share the same short 5' leader sequence, are produced by corona- and arteriviruses upon entry (Fig. 1A) (5, 16, 29). The multiplex RT-PCR assay distinguished between the mere presence of input virus, which may be nonproductive, and actual initiation of replication (entry).

Oligonucleotide RT-PCR primers were designed to amplify G3PDH and SARS-CoV gRNA and sRNA, the latter of which is indicative of virus entry and specific to initiation of SARS-CoV RNA replication (Fig. 1A). gRNA was detected by amplification of a region between the 1b coding region of the

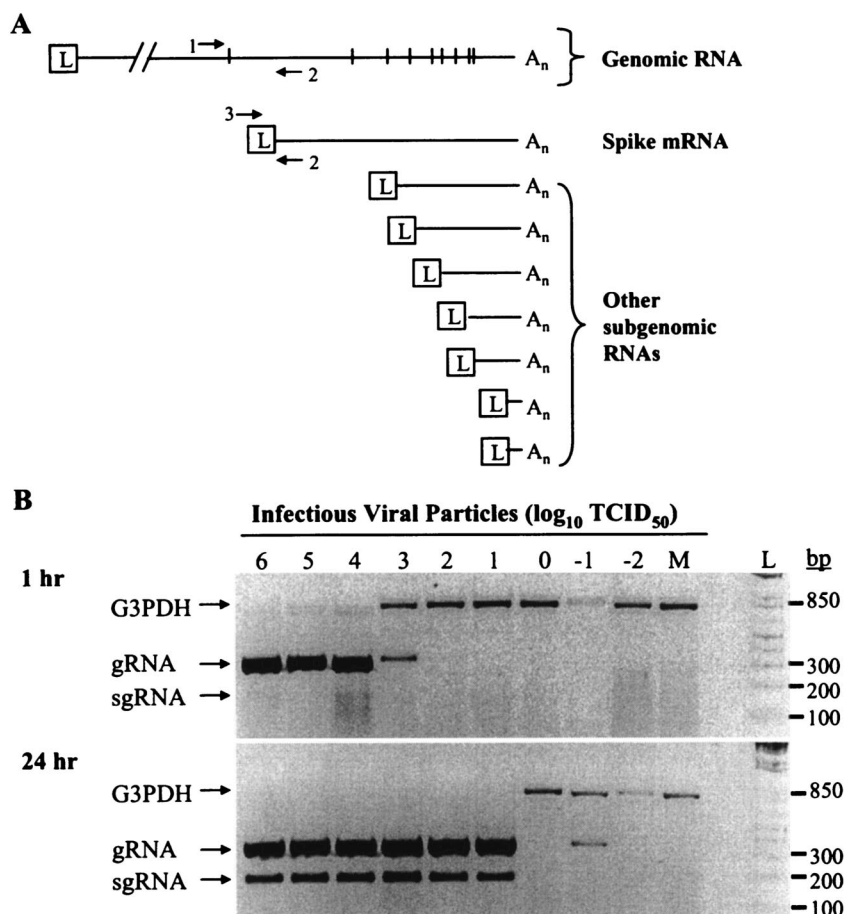


FIG. 1. Identification of SARS-CoV entry and replication initiation. (A) Schematic of CoV RNA replication and depiction of the PCR strategy used to detect SARS-CoV replication. gRNAs and sgRNAs are depicted; negative-sense sgRNAs are omitted for simplicity. L represents the short leader sequence. Oligonucleotides are depicted by the arrows. Primers 1 and 2 specifically amplify gRNA, whereas primers 2 and 3 specifically amplify spike sgRNA. (B) Approximately 1×10^6 VeroE6 cells were inoculated with serial dilutions of SARS-CoV ranging from 10^6 to 10^{-2} TCID₅₀ or were mock inoculated (M). G3PDH and SARS-CoV gRNA and sgRNA were amplified by multiplex RT-PCR of total RNA isolated at 1 or 24 h postinoculation. L denotes the molecular weight ladder. Amplicons were visualized by ethidium bromide staining after electrophoresis, and negative images are shown.

polymerase gene and the sequence encoding the S protein. sgRNA was detected by using a primer specific to the leader sequence, in conjunction with the same reverse primer in the S gene that was used for gRNA detection. G3PDH primers, designed to amplify G3PDH from multiple species, served as positive controls for RNA integrity and cDNA production.

To evaluate the multiplex RT-PCR assay, VeroE6 cells were inoculated with serial dilutions of SARS-CoV ranging from 10^6 to 10^{-2} TCID₅₀. Total RNA was extracted at 1 or 24 h postinoculation. At 1 h, input gRNA was detected in cells inoculated with 10^6 to 10^3 infectious particles, as indicated by a band at bp 300 (Fig. 1B), while sgRNA was not detected (bp 180). However, at 24 h postinoculation, both gRNA and sgRNA, at bp 300 and bp 180, respectively, were detected in cells inoculated with 10^6 to 10^1 TCID₅₀ (Fig. 1B). The sgRNA amplicon was confirmed by sequence analysis to correspond to the S sgRNA leader-body junction determined by Thiel et al. (33; data not shown). G3PDH was included as a control for RNA quality and was always detected in the absence of viral RNAs (Fig. 1B). The multiplex reaction conditions were optimized to

favor amplification of SARS-CoV RNA species at the expense of G3PDH amplification, which reduced the amplification of G3PDH when high levels of SARS-CoV gRNA and sgRNA were present (Fig. 1B). Additionally, low levels of G3PDH RNA in some samples may have been due to cell death.

Kidney cells derived from three species of monkey are susceptible to SARS-CoV. SARS-CoV has been successfully propagated in VeroE6 cells, derived from African green monkeys, and FRhMK cells, derived from fetal rhesus monkeys (14, 24). In addition, cynomolgus monkeys were the first animals tested as a model for SARS-CoV infection (9, 15). To compare kidney cells from three species of monkeys and a divergent species (Syrian hamster), VeroE6 cells, primary kidney cells derived from rhesus macaques (pRhMK) and cynomolgus macaques (pCMK), and baby hamster kidney cells (BHK-21) were inoculated with SARS-CoV (MOI ~ 0.001). SARS-CoV gRNA was detected in VeroE6, pRhMK, and pCMK cells at 1 h (input virus) and had qualitatively increased at 24 h (Fig. 2A). sgRNA, absent from input virus (1 h), was detected at 24 and 48 h in VeroE6, pRhMK and pCMK cells, indicating that

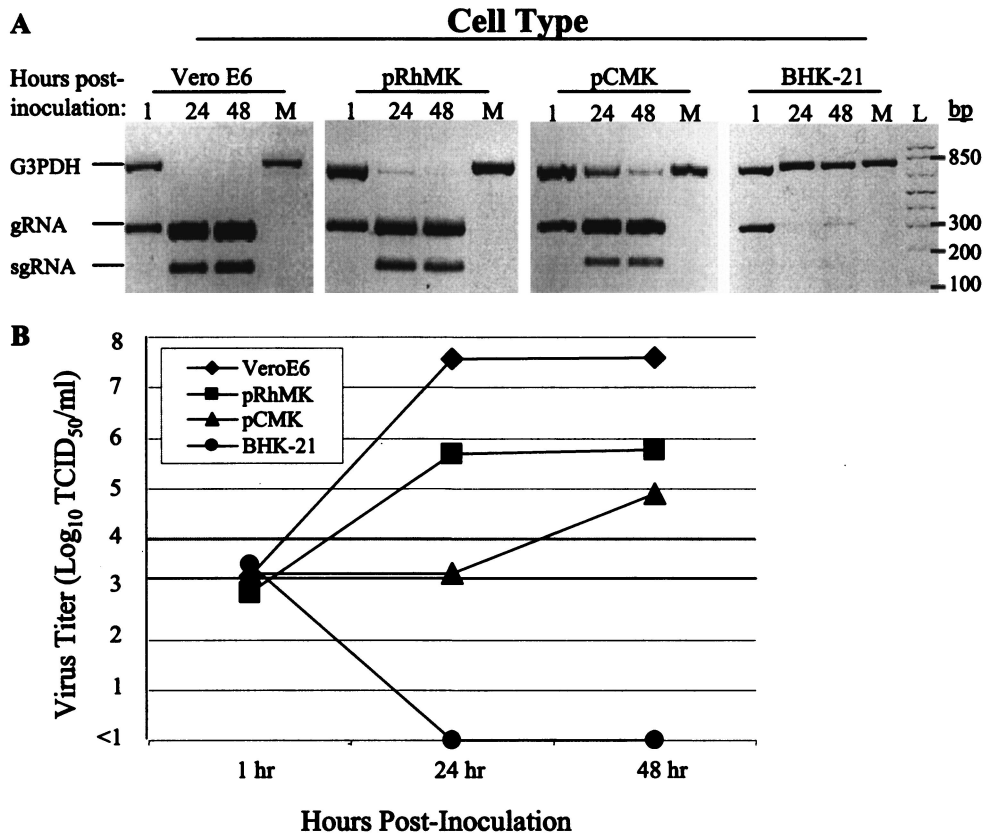


FIG. 2. Kidney cells derived from three species of monkey show differences in production of infectious SARS-CoV. African green monkey cells (VeroE6), primary rhesus monkey kidney cells (pRhMK), primary cynomolgus monkey kidney cells (pCMK), and baby hamster kidney cells (BHK-21) were inoculated with SARS-CoV at an MOI of ~0.001 or were mock inoculated (M). (A) G3PDH and SARS-CoV gRNA and sgRNA were amplified by multiplex RT-PCR in total RNA extracted at 1, 24, or 48 h postinoculation. L denotes the molecular weight ladder. Amplicons were visualized by ethidium bromide staining after electrophoresis, and negative images are shown. (B) Supernatants from inoculated cells were harvested at 1, 24, or 48 h postinoculation, and the titers of SARS-CoV were determined.

SARS-CoV initiated replication in cells from all three monkey species. In SARS-CoV-inoculated BHK-21 cells, gRNA was detected in the viral inoculum at 1 h but was not detected at 24 h (Fig. 2A). Additionally, sgRNA was not detected in these cells. G3PDH was amplified in all samples lacking gRNA and sgRNA, an indication that the RNA was intact.

The supernatants were collected, and the titers of the virus were determined at various times postinoculation to compare the amount of SARS-CoV produced by the various species. The susceptible cells demonstrated an increase in virus titer at 48 h postinoculation, whereas SARS-CoV was not detected in the supernatants from BHK-21 cells at 24 or 48 h (Fig. 2B). Interestingly, the level of SARS-CoV production differed among the three monkey species. pCMK cells demonstrated a much lower titer (2.1×10^3 TCID₅₀/ml) at 24 h than either pRhMK (4.9×10^5 TCID₅₀/ml) or VeroE6 (3.8×10^7 TCID₅₀/ml) cells. At 48 h, the titer from pCMK cells increased to 7.8×10^4 TCID₅₀/ml and the titer from pRhMK cells increased to 5.6×10^5 TCID₅₀/ml, while the titer from VeroE6 cells leveled off at 3.9×10^7 TCID₅₀/ml. Consistent with reports by Ksiazek et al., CPE was observed in VeroE6 cells at as early as 24 h (14). However, significant CPE was not observed in pRhMK or pCMK cells at 24 or 48 h or even at 5 days postinoculation

(data not shown). These data indicate that the identification of newly synthesized sgRNA is a more reliable indicator of SARS-CoV entry and replication than CPE.

Identification of clinically relevant cells permissive to SARS-CoV infection. A panel of cells routinely used by diagnostic laboratories to isolate respiratory pathogens was analyzed for susceptibility to SARS-CoV. Human embryonic lung cells (HEL) support detection of rhinovirus and respiratory syncytial virus (RSV) from clinical specimens. HEL cells were inoculated with SARS-CoV (MOI ~0.001), and the production of SARS-CoV RNA was analyzed. SARS-CoV gRNA was detected at 1 h postinoculation (input virus) but was not detected at 24 or 48 h. (Fig. 3A). sgRNA was not detectable in the inoculated HEL cells, indicating that they are nonpermissive to SARS-CoV. R-Mix supports the detection of many viruses, including influenza virus, RSV, adenovirus, and parainfluenza viruses. R-Mix was inoculated with SARS-CoV (MOI ~0.001), and the production of SARS-CoV RNA was analyzed. SARS-CoV gRNA was detected at 1, 24, and 48 h (Fig. 3A). Furthermore, detection of sgRNA at 24 and 48 h indicates that R-Mix supports entry and replication of SARS-CoV. To determine which cell(s) within R-Mix are susceptible to SARS-CoV infection, A549 and Mv1Lu cells were individ-

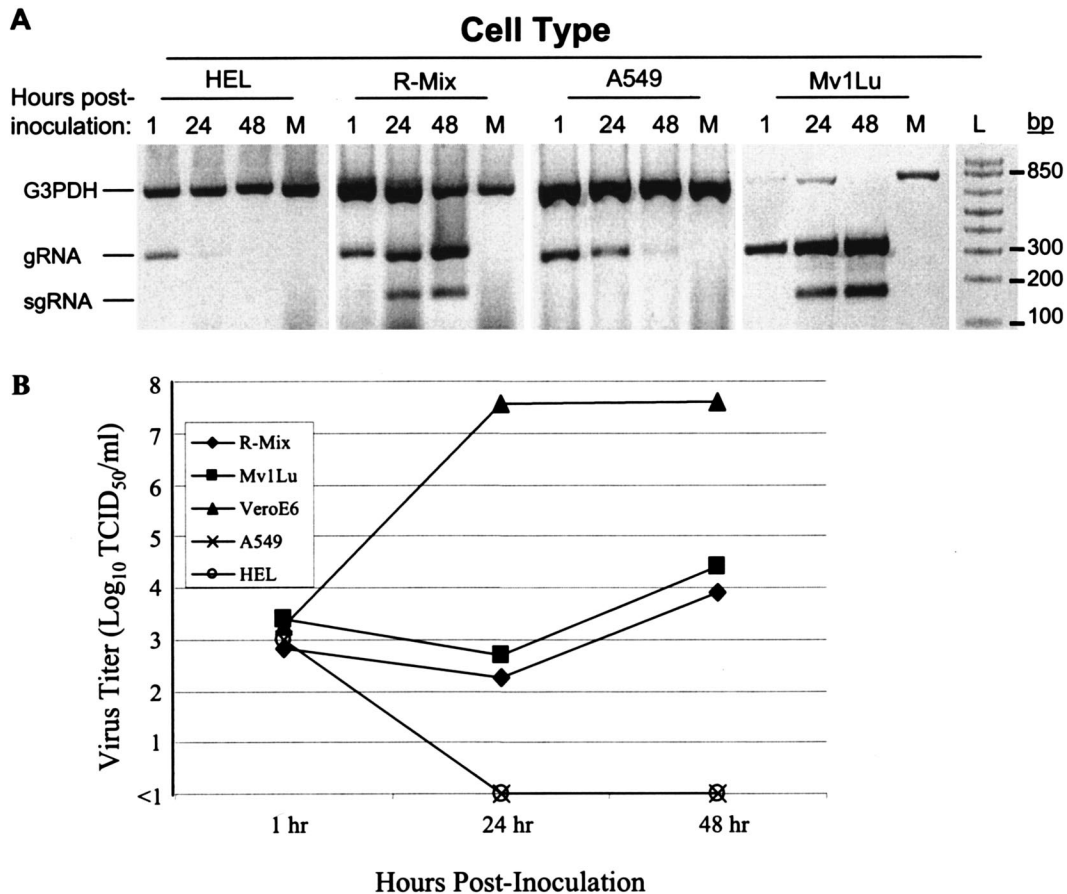


FIG. 3. Cell lines routinely used to diagnose respiratory viruses are susceptible to SARS-CoV. HEL cells, R-Mix cells, human lung cells (A549), and Mv1Lu cells were inoculated with SARS-CoV at an MOI of ~ 0.001 or were mock inoculated (M). (A) G3PDH and SARS-CoV gRNA and sgRNA were amplified by multiplex RT-PCR in total RNA extracted at 1, 24, or 48 h postinoculation. L denotes the molecular weight ladder. Amplicons were visualized by ethidium bromide staining after electrophoresis, and negative images are shown. (B) The supernatants from inoculated cells were harvested at 1, 24, or 48 h postinoculation, and the titers of SARS-CoV were determined by TCID₅₀.

ually examined postinoculation (MOI ~ 0.001). SARS-CoV gRNA was detected in A549 cells at 1, 24, and 48 h (Fig. 3A). However, sgRNA was not detectable in these cells, indicating that they do not support SARS-CoV replication. In contrast, sgRNA was detectable in Mv1Lu cells at 24 and 48 h (Fig. 3A), which shows that Mv1Lu cells are the cell population within R-Mix that are infected with SARS-CoV. Viral titers in both R-Mix and Mv1Lu increased from $\sim 1 \times 10^3$ TCID₅₀/ml at 24 h to $\sim 1 \times 10^4$ TCID₅₀/ml at 48 h, while titers in the supernatants from A549 cells decreased below the level of detection at 24 h (Fig. 3B). In contrast, VeroE6 cell supernatants contained 4 log₁₀ more SARS-CoV than R-Mix and Mv1Lu cells at 24 h (Fig. 3B). Virus titers in HEL supernatants were below the limit of detection at 24 h. These results show that SARS-CoV productively infects Mv1Lu cells; however, production of infectious virus is much lower in these cells than that observed in VeroE6 cells. Taken together, the data indicate that Mv1Lu cells, routinely used by clinical laboratories, are susceptible to SARS-CoV, although they produce dramatically less virus than VeroE6 cells. These cells may provide a safer diagnostic substrate than VeroE6 cells.

Analysis of cells expressing known coronavirus receptors. Cell lines known to be susceptible to other CoVs were assayed for their susceptibility to SARS-CoV. Cells infected by human, feline, canine, avian, and murine CoVs were inoculated with SARS-CoV and analyzed for viral replication. The cells examined included human lung fibroblast-derived cells (MRC-5), canine kidney-derived cells (MDCK), and feline lung epithelium cells (AK-D). These cells are susceptible to HCoV-229E, canine CoVs, and feline CoVs, respectively. Cells permissive to group 2 CoVs, including mouse fibroblast-derived cells (L2) that express the receptor utilized by strains of MHV (CEACAM1a) and a human rectal tumor cell line (HRT-18) known to be susceptible to HCoV-OC43 and bovine CoV, were analyzed. CEF cells permissive to group 3 CoV infectious bronchitis virus were also tested. Although SARS-CoV gRNA was amplified in all six cell lines at 1 h and persisted in some cell lines to 48 h, it appeared to decrease over the time course (Fig. 4). Furthermore, sgRNA was not detectable at any time postinoculation, indicating that these cells are not permissive to SARS-CoV infection. sgRNA was detected in VeroE6 cells included as positive controls. These data illustrate that SARS-

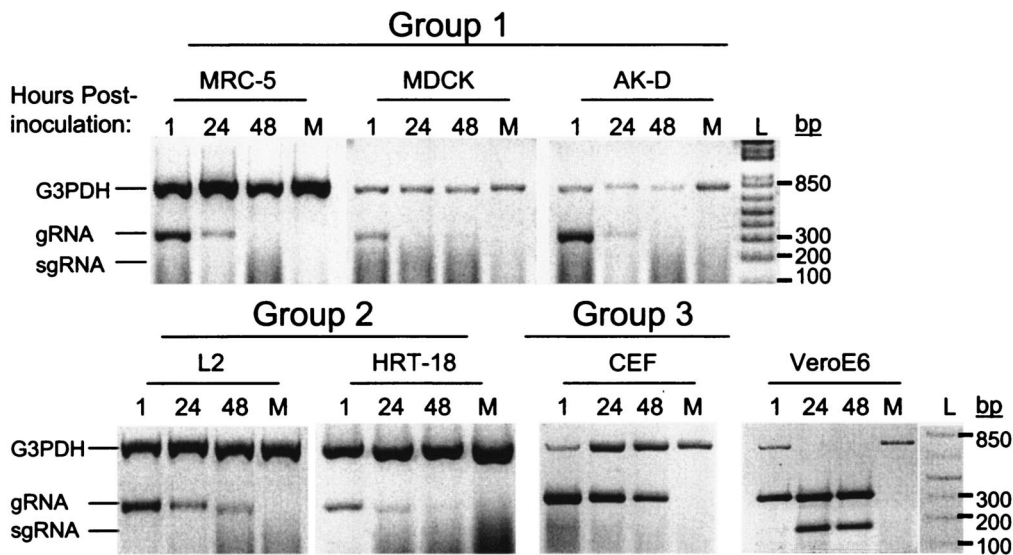


FIG. 4. Cell lines susceptible to group 1, 2, and 3 coronaviruses are not permissive to SARS-CoV infection. Human lung fibroblasts (MRC-5), canine kidney cells (MDCK), feline lung epithelium cells (AK-D), murine fibroblasts (L2), human rectal tumor cells (HRT-18), CEFs, and VeroE6 cells were inoculated with SARS-CoV at an MOI of ~0.001 or were mock inoculated (M). G3PDH and SARS-CoV gRNA and sgRNA were amplified by multiplex RT-PCR from total RNA extracted at 1, 24, or 48 h postinoculation. L denotes the molecular weight ladder. Amplicons were visualized by ethidium bromide staining after electrophoresis, and negative images are shown.

CoV cannot exploit cellular receptors used by other CoVs of groups 1, 2, and 3 or that there is a postentry block to viral replication in these cells.

Identification of human cell lines permissive to SARS-CoV infection. Although humans are infected by SARS-CoV, human-derived cell lines that efficiently produce SARS-CoV have not been demonstrated (6, 14, 24). SARS-CoV has been detected in human tissues, including lung, kidney, liver, and PBMCs (14, 17, 24). Based on these findings, human embryonic kidney (HEK-293T) cells and human liver (Huh-7) cells were inoculated with SARS-CoV (MOI ~0.001) to determine their susceptibility. MRC-5 cells, a cell line derived from human lung and previously determined to be nonpermissive to SARS-CoV (Fig. 4), were included as negative controls (24). SARS-CoV gRNA was detected at 1 h (input virus), and an increase in its level was apparent at 24 and 48 h in both HEK-293T and Huh-7 cells (Fig. 5A). Newly synthesized sgRNA was detectable at 24 and 48 h in both HEK-293T and Huh-7 cells, whereas MRC-5 cells were negative for sgRNA at all time points. These data show that HEK-293T and Huh-7 cells express the appropriate receptor for SARS-CoV and are permissive to SARS-CoV RNA replication. To determine whether HEK-293T and Huh-7 cells are productively infected by SARS-CoV, titers of the virus in the supernatants collected at all time points were determined. At 24 h, HEK-293T cell supernatants contained 3.2×10^3 TCID₅₀/ml and those of Huh-7 contained 2.4×10^4 TCID₅₀/ml (Fig. 5B). At 48 h, SARS-CoV increased to 3.7×10^3 and 1.6×10^5 TCID₅₀/ml, respectively, in HEK-293T and Huh-7 cell supernatants. VeroE6 cell supernatants contained 3.9×10^7 TCID₅₀/ml (Fig. 5B). CPE was apparent at 24 h in VeroE6 cells; however, CPE was not observed in HEK-293T or Huh-7 cells at 48 h after SARS-CoV inoculation. These results show that two human

cell lines are productively infected by SARS-CoV but that they produce less infectious virus than VeroE6 cells.

Analysis of the importance of APN in SARS-CoV entry. APN, the receptor for many group 1 CoVs, is expressed by epithelial cells of the respiratory and intestinal tracts. Furthermore, APN is expressed at high levels in the kidney and liver, organs from which SARS-CoV has been isolated. All cells that were permissive to SARS-CoV likely expressed APN, as they were derived from kidney, liver, lung, or PBMCs. To more stringently test the role of hAPN in SARS-CoV entry, cells expressing high levels of hAPN on their surfaces were tested for susceptibility to infection with SARS-CoV. A murine epithelium cell line (CMT-93) and BHK-21 cells were transfected with a construct expressing hAPN to yield CMT-93/hAPN and BHK-21/hAPN (35). CMT-93 and BHK-21 cells are nonpermissive to HCoV-229E infection and replication; however, they become permissive to HCoV-229E upon transfection and expression of hAPN (35). CMT-93/hAPN is a clonal cell line that expresses approximately five times the level of hAPN on the cell surface than is expressed by MRC-5 cells, while the BHK-21/hAPN line is a mixed population of stably transfected cells that express a wide range of hAPN levels (from below the limit of detection to 10 times that of MRC-5). hAPN was expressed at high levels on both CMT-93/hAPN and BHK-21/hAPN cells, as demonstrated by FACS analysis (Fig. 6A). Additionally, Huh-7 cells also express high levels of hAPN. Although SARS-CoV gRNA was detected in CMT-93, CMT-93/hAPN, BHK-21, and BHK-21/hAPN cells postinoculation, sgRNA was not detected at any time point (Fig. 6B). Thus, all four cell lines were nonpermissive for SARS-CoV replication, irrespective of the expression of hAPN. This data shows that expression of hAPN is not sufficient for SARS-CoV entry.

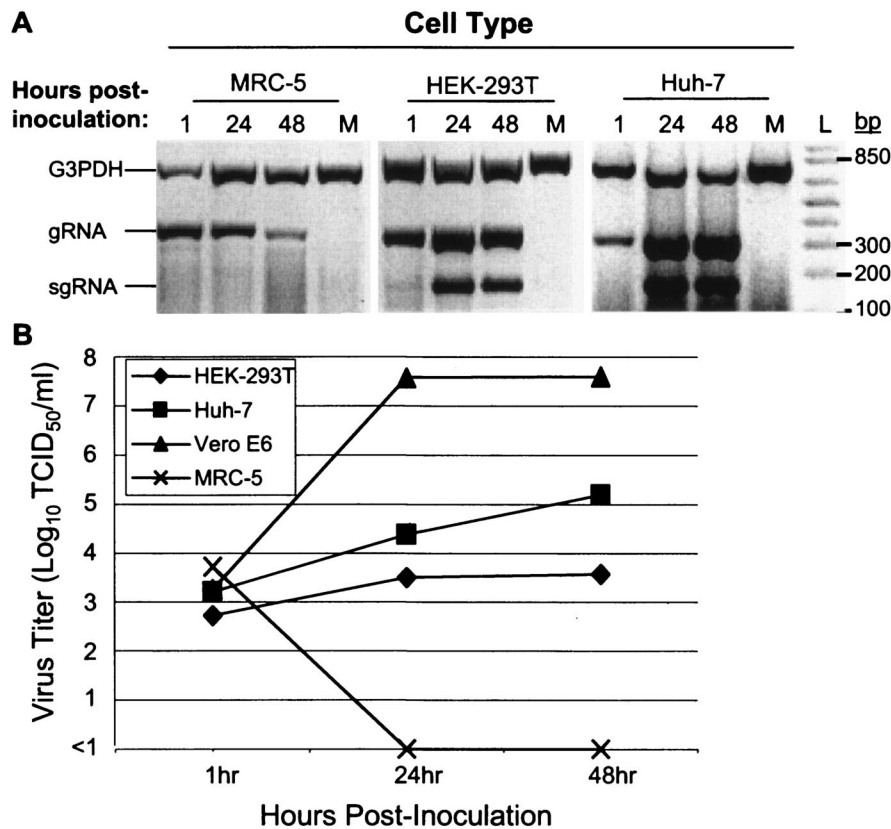


FIG. 5. Discovery of human cell lines susceptible to SARS-CoV. Cells derived from human lung fibroblasts (MRC-5), human embryonic kidneys (HEK-293T), and human livers (Huh-7) were inoculated with SARS-CoV at an MOI of ~ 0.001 or were mock inoculated (M). (A) G3PDH and SARS-CoV gRNA and sgRNA were amplified by multiplex RT-PCR from total RNA extracted at 1, 24, or 48 h postinoculation. L denotes the molecular weight ladder. Amplicons were visualized by ethidium bromide staining after electrophoresis, and negative images are shown. (B) The supernatants from inoculated cells were harvested at 1, 24, or 48 h postinoculation, and the titers of SARS-CoV were determined.

DISCUSSION

This study was designed to analyze the species specificity and tissue tropism of SARS-CoV *in vitro* and to identify novel human and animal cells that are susceptible to SARS-CoV infection. The multiplex RT-PCR assay described rapidly and specifically detects early replication of SARS-CoV RNA and is an indirect measure of viral entry (Fig. 1B). Importantly, this assay can identify cells that are susceptible to SARS-CoV entry and RNA transcription yet result in minimal CPE or that have blocks between RNA transcription and the efficient production of progeny viruses (Table 1). Previously described RT-PCR procedures detect SARS-CoV gRNA; however, the detection of sgRNA production described here provides an effective approach to differentiate input virus from replicating virus (6, 25, 26, 37). This assay may be useful in a diagnostic setting and for the analysis of animal models. In addition, it could be used to screen for potential inhibitors of viral replication.

Previously published reports predicted that all monkey kidney cells would be susceptible to SARS-CoV (6, 14, 24, 26). In agreement with previous findings, the data presented here show that kidney cells derived from three species of monkey (African green monkey, rhesus macaque, and cynomolgus macaque) are productively infected with SARS-CoV. Fouchier et al. and Kuiken et al. demonstrated that cynomolgus macaques

inoculated with SARS-CoV develop clinical symptoms consistent with infection (9, 15). Although SARS-CoV was not detected in the kidneys of these animals by immunohistochemical techniques, our data coupled with work by Ksiazek et al. suggests that the kidney supports SARS-CoV replication (14). Evaluation of these tissues with more-sensitive methods may identify SARS-CoV in the kidneys of experimentally infected animals. Interestingly, infection of pCMK and pRhMK cells resulted in lower viral titers than infection of VeroE6 cells. The reason for these results remains to be determined, but a potential explanation is that VeroE6 is a cell line deficient in interferon production, whereas pCMK and pRhMK are both primary cell populations. Additionally, pCMK and pRhMK are both mixed cell populations; thus, the cells susceptible to SARS-CoV may make up only a percentage of the total cell population.

At the beginning of the SARS-CoV outbreak, panels of cells were inoculated with clinical specimens to identify the causative agent of SARS (6, 14, 24). Based on CPE, VeroE6 and FRhMK cells were identified as susceptible to SARS-CoV infection (6, 14, 24). However, many CoVs can establish persistent infection in cells without inducing CPE, and we have detected replication of SARS-CoV in the absence of CPE (11). The analysis of SARS-CoV infection of cells that are routinely

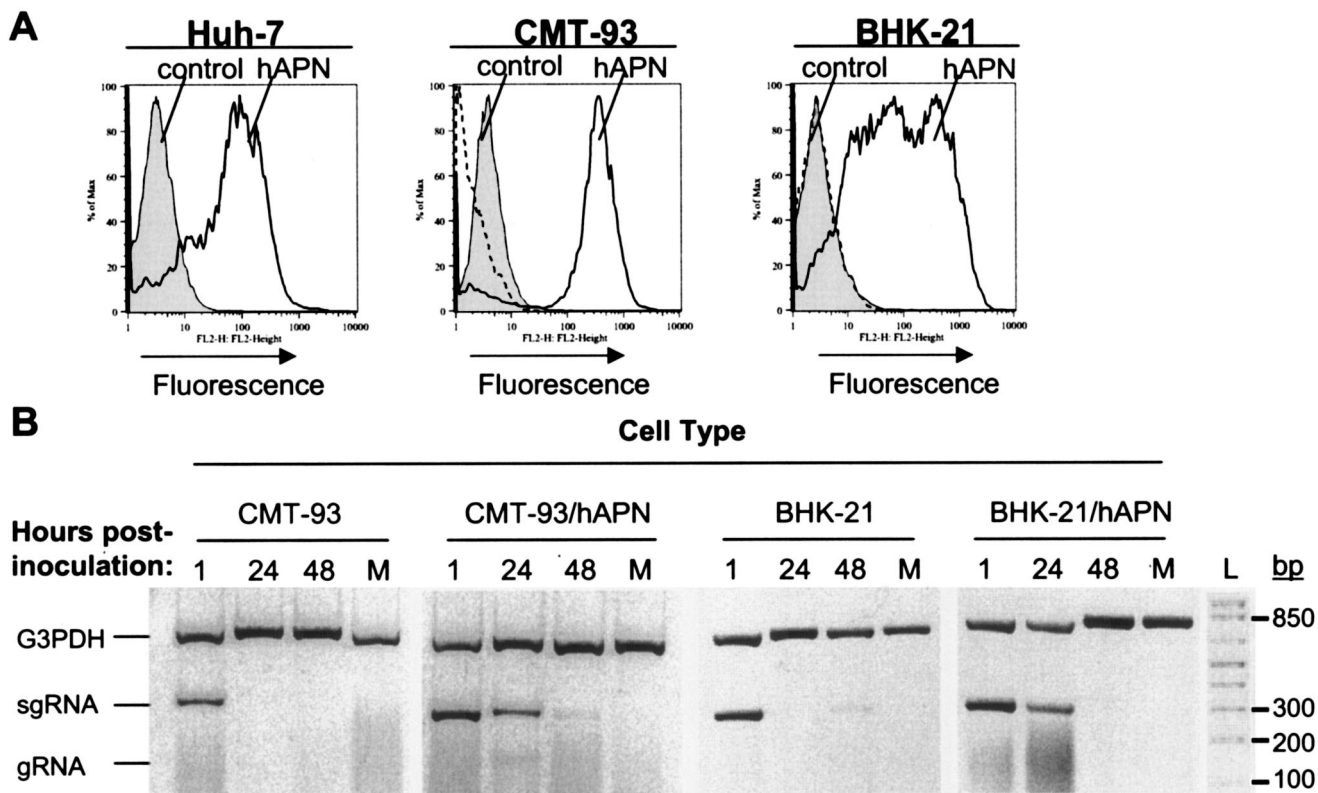


FIG. 6. hAPN is not sufficient for SARS-CoV entry. (A) FACS analysis of hAPN expression. Cells derived from human livers (Huh-7), murine epithelia (CMT-93), a clone of CMT-93 expressing hAPN (CMT-93/hAPN), baby hamster kidney cells (BHK-21), and BHK-21 cells expressing hAPN (BHK-21/hAPN) were labeled with a monoclonal antibody that recognizes hAPN (DW-1). Cells transfected with hAPN are represented by the solid line, cells without transfected APN are represented by the dashed line, and staining with isotype control antibody (mouse immunoglobulin G2) is represented by the shaded curve. (B) CMT-93, CMT-93/hAPN, BHK-21, and BHK-21/hAPN cells were inoculated with SARS-CoV at an MOI of ~0.001 or were mock inoculated (M). G3PDH and SARS-CoV gRNA and sgRNA were amplified by multiplex RT-PCR from total RNA extracted at 1, 24, or 48 h postinoculation. L denotes the molecular weight ladder. Amplicons were visualized by ethidium bromide staining after electrophoresis, and negative images are shown.

used by clinical virology laboratories is critical from both biological safety and diagnostic standpoints. The clinical presentation of SARS-CoV infection is very similar to that of influenza virus and other respiratory pathogens. Given the possibility for SARS-coronavirus re-emergence to occur during influenza or other respiratory disease seasons, it is important to identify cells used by clinical laboratories that support SARS-CoV replication so that SARS-CoV is not inadvertently produced without appropriate biosafety precautions. A panel of cells used to isolate respiratory viruses was analyzed for susceptibility to SARS-CoV. MRC-5, HEL, and A549 cells, lung-derived cells used to screen specimens for rhinovirus, RSV, adenovirus, and influenza virus, were nonpermissive to SARS-CoV replication based on the multiplex RT-PCR assay. However, R-Mix, a mixed cell population used for the detection of influenza A and B viruses, RSV, adenovirus, and parainfluenza viruses 1, 2, and 3, was found to be productively infected by SARS-CoV. We identified Mv1Lu as the cell population within R-Mix that supports productive SARS-CoV infection. Despite the low yield of SARS-CoV in Mv1Lu and R-Mix cells, their widespread use in clinical diagnostic laboratories warrants further work to devise methods of enhancing their safety. Ongoing approaches include the incorporation of

SARS-CoV-specific monoclonal antibodies or antiviral agents into the maintenance medium and determining the effect medium components have on SARS-CoV replication. Diagnostic laboratories utilizing R-Mix and Mv1Lu for the detection of respiratory specimens perform inoculations in medium that contains different components from those of the medium used in this study (e.g., it lacks FBS and contains trypsin). Additional evaluation of the susceptibility of these cell lines is being carried out under conditions utilized by clinical laboratories, as they may provide enhanced safeguards against amplification of SARS-CoV. Preliminary evidence strongly suggests that the passage history and/or medium components during passage or infection alter the production of SARS-CoV by Mv1Lu cells (data not shown). Our results demonstrate the importance of conducting further work to analyze cells used to diagnose illnesses that have clinical symptoms similar to those of influenza virus and SARS-CoV infection. For example, rhesus monkey kidney cells (LLC-MK2), used for the detection of rhinovirus, did not show CPE when inoculated with a clinical SARS-CoV specimen (14). However, both pRhMK and FRhMK cells are susceptible to SARS-CoV, suggesting that LLC-MK2 cells may also be susceptible (24). The discovery that Mv1Lu cells are permissive to SARS-CoV infection is also important in the

TABLE 1. Susceptibility of cells to SARS-CoV

| Cell line or type | Species of origin | SARS-CoV sgRNA ^d | CPE ^d | Titer ^a |
|-------------------|----------------------|-----------------------------|------------------|--------------------|
| VeroE6 | African green monkey | + | + | 2.4×10^7 |
| pRhMK | Rhesus macaque | + | – | 5.6×10^5 |
| pCMK | Cynomolgus macaque | + | – | 7.8×10^4 |
| R-Mix | Mink and human | + | – | 7.8×10^3 |
| A549 | Human | – | – | <1 ^b |
| Mv1Lu | Mink | + | – | 2.5×10^4 |
| HEL | Human | – | – | <1 |
| MRC-5 | Human | – | – | <1 |
| MDCK | Canine | – | – | <1 |
| AK-D | Feline | – | – | ND ^c |
| L2 | Murine | – | – | ND ^c |
| HRT-18 | Human | – | – | ND ^c |
| CEF | Chicken | – | – | ND ^c |
| HEK-293T | Human | + | – | 5.6×10^3 |
| Huh-7 | Human | + | – | 1.3×10^5 |
| CMT-93 | Murine | – | – | ND ^c |
| CMT-93/hAPN | Murine | – | – | ND ^c |
| BHK-21 | Syrian hamster | – | – | <1 |
| BHK-21/hAPN | Syrian hamster | – | – | <1 |

^a TCID₅₀/ml at 48 h postinfection.

^b Below the limit of detection.

^c Not determined.

^d +, susceptible; –, not susceptible.

development of safer diagnostic assays, identification of receptors, and understanding of the virus life cycle and also suggests that mink and other related species are potential animal models or natural reservoirs (10, 20).

To investigate the possibility that cellular receptors utilized by other CoVs could function as receptors for SARS-CoV, cell lines known to be permissive to CoVs from groups 1, 2, and 3 were analyzed by multiplex RT-PCR for SARS-CoV RNA replication. APN (also called CD13), is a 150-kDa metalloprotease that serves as a receptor for related CoVs of humans (HCoV-229E), pigs (transmissible gastroenteritis virus and porcine respiratory coronavirus), and cats (feline infectious peritonitis virus and feline coronavirus) (4, 34, 38). APN is expressed in tissues such as the liver and kidney, as well as on granulocytes, monocytes, dendritic cells, and endothelial cells and by epithelial cells of the intestine and respiratory tract, where it allows initial entry of CoVs (22, 27). To examine the potential involvement of hAPN in SARS-CoV entry, we inoculated human lung cells, canine kidney cells, and feline lung cells that are productively infected by HCoV-229E, canine CoV, and feline CoVs, respectively. In agreement with Ksiazek et al., no evidence of SARS-CoV entry was observed (14). Furthermore, cells derived from two other species (mouse and hamster) expressing high levels of hAPN and previously demonstrated to be susceptible to HCoV-229E were also demonstrated to be nonpermissive to SARS-CoV (35). These results show that hAPN is not sufficient for entry of SARS-CoV. Similar results were found by K. V. Holmes and collaborators (personal communication). SARS-CoV is most closely related to group 2 CoVs, suggesting that it may use a receptor utilized by another group 2 CoV (32). However, murine cells expressing CEACAM1a (L2 and CMT-93), the receptor for MHV, and HRT-18 cells, which are susceptible to HCoV-OC43 and bovine CoV, were both found to be nonpermissive to SARS-CoV infection. Finally, avian cells susceptible to a group 3 avian CoV (CEF) were also found to be nonpermissive for

SARS-CoV infection. These data are in agreement with a recent study that shows that angiotensin-2-converting enzyme is a functional receptor for SARS-CoV (18).

The SARS-CoV outbreak affected the human population, yet human cell lines productively infected by SARS-CoV were not demonstrated prior to this study. We examined human cell lines derived from lung (HEL A549 and MRC-5), intestine (HRT-18), kidney (HEK-293T), and liver (Huh-7). HEL, MRC-5, and HRT-18 cells were all nonpermissive to SARS-CoV infection; however, we identified two susceptible human-derived cell lines, HEK-293T and Huh-7. Huh-7 is a hepatocellular carcinoma cell line that is widely utilized to study hepatitis B and C viruses. Our results indicate that Huh-7 cells are productively infected by SARS-CoV and that they produce higher levels of virus than do HEK-293T cells. Interestingly, Huh-7 cells were previously shown to be susceptible to the DL and DS variants of MHV-JHM, a neurotropic group 2 CoV (12). Furthermore, infection of Huh-7 cells by JHM was mediated by the S protein (12). A Blastp GenBank search with the predicted amino acid sequence of the SARS-CoV S protein reveals that it shares the most amino acid similarity with the S protein of MHV-JHM (1, 31). MHV-JHM utilizes murine CEACAM1a as a primary receptor, but it is one of very few isolates of MHV that has shown a broader host range (2, 12, 21, 30), which leads to the possibility that conserved amino acids or motifs in the S protein of JHM and SARS-CoV interact with the receptor on host cells.

The susceptibility of HEK-293T cells correlates with the susceptibility of primate kidney cells to SARS-CoV and the isolation of SARS-CoV from the kidney of an infected patient (14). While HEK-293T and Huh-7 cells are susceptible to SARS-CoV infection, HEK-293T cells do not produce high titers of virus when inoculated with a low multiplicity of virus. The reason for this low level of virus production remains to be determined but may be due to low-level surface expression of angiotensin-2-converting enzyme (18). Like Mv1Lu cells,

HEK-293T cells may provide a safer diagnostic alternative to VeroE6 cells, which produce >10,000-fold-greater titers of SARS-CoV.

The data presented here are important to vaccine production, diagnostic assay development, and elucidation of animal models and reservoirs susceptible to SARS-CoV. Furthermore, the data suggest that other human and animal cells are likely to be susceptible to SARS-CoV upon examination and that laboratories may need to adopt different practices to prevent accidental exposure to SARS-CoV during routine screening of clinical specimens.

Coronaviruses tend to be species specific, yet SARS-CoV appears to have crossed species barriers and infected humans, resulting in high morbidity and mortality (10, 23, 39). Our *in vitro* data, in conjunction with data from multiple animal studies, show that SARS-CoV has a broad host range (9, 10, 15, 20), which suggests that SARS-CoV or closely related variants may be circulating in multiple animal reservoirs, increasing the likelihood of its re-emergence in humans.

ACKNOWLEDGMENTS

D.E.W. thanks Kathryn V. Holmes for the anti-hAPN monoclonal antibodies (DW-1) and hAPN clones that resulted from previous studies together. The authors thank Noel Espina for his expert assistance with cell culture and molecular biology and the Wadsworth Center Molecular Genetics Core for DNA sequencing and oligonucleotide synthesis.

L.G.-R. was supported as an appointee to the Emerging Infectious Disease (EID) Fellowship Program administered by the Association of Public Health Laboratories and funded by the Centers for Disease Control and Prevention. J.T., D.E.W., and supplies were funded by the Public Health Preparedness and Response to Bioterrorism cooperative agreement between the Department of Health and Human Services and the Centers for Disease Control and Prevention (U901CCU216988-03). This work was also supported in part by federal funds from the National Institute of Allergy and Infectious Diseases, NIH, under contract number N01-A1-25490.

REFERENCES

- Altschul, S. F., and E. V. Koonin. 1998. Iterated profile searches with PSI-BLAST—a tool for discovery in protein databases. *Trends Biochem. Sci.* 23:444–447.
- Baric, R. S., E. Sullivan, L. Hensley, B. Yount, and W. Chen. 1999. Persistent infection promotes cross-species transmissibility of mouse hepatitis virus. *J. Virol.* 73:638–649.
- Compton, S. R., C. B. Stephensen, S. W. Snyder, D. G. Weismiller, and K. V. Holmes. 1992. Coronavirus species specificity: murine coronavirus binds to a mouse-specific epitope on its carcinoembryonic antigen-related receptor glycoprotein. *J. Virol.* 66:7420–7428.
- Delmas, B., J. Gelfi, R. L'Haridon, L. K. Vogel, H. Sjoström, O. Noren, and H. Laude. 1992. Aminopeptidase N is a major receptor for the enteropathogenic coronavirus TGEV. *Nature* 357:417–420.
- den Boon, J. A., M. F. Kleijnen, W. J. Spaan, and E. J. Snijder. 1996. Equine arteritis virus subgenomic mRNA synthesis: analysis of leader-body junctions and replicative-form RNAs. *J. Virol.* 70:4291–4298.
- Drosten, C., S. Gunther, W. Preiser, S. van der Werf, H. R. Brodt, S. Becker, H. Rabenau, M. Panning, L. Kolesnikova, R. A. Fouchier, A. Berger, A. M. Burguiere, J. Cinatl, M. Eickmann, N. Escriou, K. Grywna, S. Kramme, J. C. Manuguerra, S. Müller, V. Ricketts, M. Stürmer, S. Vieth, H. D. Klenk, A. D. Osterhaus, H. Schmitz, and H. W. Doerr. 2003. Identification of a novel coronavirus in patients with severe acute respiratory syndrome. *N. Engl. J. Med.* 348:1967–1976.
- Dveksler, G. S., S. E. Gagneten, C. A. Scanga, C. B. Cardellicchio, and K. V. Holmes. 1996. Expression of the recombinant anchorless N-terminal domain of mouse hepatitis virus (MHV) receptor makes hamster or human cells susceptible to MHV infection. *J. Virol.* 70:4142–4145.
- Dveksler, G. S., M. N. Pensiero, C. B. Cardellicchio, R. K. Williams, G. S. Jiang, K. V. Holmes, and C. W. Dieffenbach. 1991. Cloning of the mouse hepatitis virus (MHV) receptor: expression in human and hamster cell lines confers susceptibility to MHV. *J. Virol.* 65:6881–6891.
- Fouchier, R. A., T. Kuiken, M. Schutten, G. van Amerongen, G. J. van Doornum, B. G. van den Hoogen, M. Peiris, W. Lim, K. Stohr, and A. D. Osterhaus. 2003. Aetiology: Koch's postulates fulfilled for SARS virus. *Nature* 423:240.
- Guan, Y., B. J. Zheng, Y. Q. He, X. L. Liu, Z. X. Zhuang, C. L. Cheung, S. W. Luo, P. H. Li, L. J. Zhang, Y. J. Guan, K. M. Butt, K. L. Wong, K. W. Chan, W. Lim, K. F. Shortridge, K. Y. Yuen, J. S. Peiris, and L. L. Poon. 2003. Isolation and characterization of viruses related to the SARS coronavirus from animals in southern China. *Science* 302:276–278.
- Holmes, K. V. 2001. Coronaviruses, p. 1187–1203. *In* D. M. Knipe and P. M. Howley (ed.), *Fields virology*. Lippincott-Raven, Philadelphia, Pa.
- Koetters, P. J., L. Hassanieh, S. A. Stohman, T. Gallagher, and M. M. Lai. 1999. Mouse hepatitis virus strain JHM infects a human hepatocellular carcinoma cell line. *Virology* 264:398–409.
- Kolb, A. F., A. Hegyi, and S. G. Siddell. 1997. Identification of residues critical for the human coronavirus 229E receptor function of human aminopeptidase N. *J. Gen. Virol.* 78:2795–2802.
- Ksiazek, T. G., D. Erdman, C. S. Goldsmith, S. R. Zaki, T. Peret, S. Emery, S. Tong, C. Urbani, J. A. Comer, W. Lim, P. E. Rollin, S. F. Dowell, A. E. Ling, C. D. Humphrey, W. J. Shieh, J. Guarner, C. D. Paddock, P. Rota, B. Fields, J. DeRisi, J. Y. Yang, N. Cox, J. M. Hughes, J. W. LeDuc, W. J. Bellini, and L. J. Anderson. 2003. A novel coronavirus associated with severe acute respiratory syndrome. *N. Engl. J. Med.* 348:1953–1966.
- Kuiken, T., R. A. Fouchier, M. Schutten, G. F. Rimmelzwaan, G. van Amerongen, D. van Riel, J. D. Laman, T. de Jong, G. van Doornum, W. Lim, A. E. Ling, P. K. Chan, J. S. Tam, M. C. Zambon, R. Gopal, C. Drosten, S. van der Werf, N. Escriou, J. C. Manuguerra, K. Stohr, J. S. Peiris, and A. D. Osterhaus. 2003. Newly discovered coronavirus as the primary cause of severe acute respiratory syndrome. *Lancet* 362:263–270.
- Lai, M. M., and K. V. Holmes. 2001. Coronaviridae: the viruses and their replication, p. 1163–1186. *In* D. M. Knipe and P. M. Howley (ed.), *Fields virology*. Lippincott-Raven, Philadelphia, Pa.
- Li, L., J. Wo, J. Shao, H. Zhu, N. Wu, M. Li, H. Yao, M. Hu, and R. H. Dennin. 2003. SARS-coronavirus replicates in mononuclear cells of peripheral blood (PBMCs) from SARS patients. *J. Clin. Virol.* 28:239–244.
- Li, W., M. J. Moore, N. Vasilieva, J. Sui, S. K. Wong, M. A. Berne, M. Somasundaran, J. L. Sullivan, K. Luzuriaga, T. C. Greenough, H. Choe, and M. Farzan. 2003. Angiotensin-converting enzyme 2 is a functional receptor for the SARS coronavirus. *Nature* 426:450–454.
- Marra, M. A., S. J. Jones, C. R. Astell, R. A. Holt, A. Brooks-Wilson, Y. S. Butterfield, J. Khattri, J. K. Asano, S. A. Barber, S. Y. Chan, A. Cloutier, S. M. Coughlin, D. Freeman, N. Girm, O. L. Griffith, S. R. Leach, M. Mayo, H. McDonald, S. B. Montgomery, P. K. Pandoh, A. S. Petrescu, A. G. Robertson, J. E. Schein, A. Siddiqui, D. E. Smailus, J. M. Stott, G. S. Yang, F. Plummer, A. Donovon, H. Artsob, N. Bastien, K. Bernard, T. F. Booth, D. Bowness, M. Czub, M. Drebot, L. Fernando, R. Flick, M. Garbutt, M. Gray, A. Grolla, S. Jones, H. Feldmann, A. Meyers, A. Kabani, Y. Li, S. Normand, U. Stroher, G. A. Tipples, S. Tyler, R. Vogrig, D. Ward, B. Watson, R. C. Brunham, M. Kraiden, M. Petric, D. M. Skowronski, C. Upton, and R. L. Roper. 2003. The genome sequence of the SARS-associated coronavirus. *Science* 300:1399–1404.
- Martina, B. E., B. L. Haagmans, T. Kuiken, R. A. Fouchier, G. F. Rimmelzwaan, G. van Amerongen, J. S. Peiris, W. Lim, and A. D. Osterhaus. 2003. Virology: SARS virus infection of cats and ferrets. *Nature* 425:915.
- Murray, R. S., G. Y. Cai, K. Hoel, J. Y. Zhang, K. F. Soike, and G. F. Cabirac. 1992. Coronavirus infects and causes demyelination in primate central nervous system. *Virology* 188:274–284.
- Noren, K., G. H. Hansen, H. Clausen, O. Noren, H. Sjoström, and L. K. Vogel. 1997. Defectively N-glycosylated and non-O-glycosylated aminopeptidase N (CD13) is normally expressed at the cell surface and has full enzymatic activity. *Exp. Cell Res.* 231:112–118.
- Peiris, J. S., C. M. Chu, V. C. Cheng, K. S. Chan, I. F. Hung, L. L. Poon, K. I. Law, B. S. Tang, T. Y. Hon, C. S. Chan, K. H. Chan, J. S. Ng, B. J. Zheng, W. L. Ng, R. W. Lai, Y. Guan, and K. Y. Yuen. 2003. Clinical progression and viral load in a community outbreak of coronavirus-associated SARS pneumonia: a prospective study. *Lancet* 361:1767–1772.
- Peiris, J. S., S. T. Lai, L. L. Poon, Y. Guan, L. Y. Yam, W. Lim, J. Nicholls, W. K. Yee, W. W. Yan, M. T. Cheung, V. C. Cheng, K. H. Chan, D. N. Tsang, R. W. Yung, T. K. Ng, and K. Y. Yuen. 2003. Coronavirus as a possible cause of severe acute respiratory syndrome. *Lancet* 361:1319–1325.
- Poon, L. L., O. K. Wong, K. H. Chan, W. Luk, K. Y. Yuen, J. S. Peiris, and Y. Guan. 2003. Rapid diagnosis of a coronavirus associated with severe acute respiratory syndrome (SARS). *Clin. Chem.* 49:953–955.
- Poutanen, S. M., D. E. Low, B. Henry, S. Finkelstein, D. Rose, K. Green, R. Tellier, R. Draker, D. Adachi, M. Ayers, A. K. Chan, D. M. Skowronski, I. Salit, A. E. Simor, A. S. Slutsky, P. W. Doyle, M. Kraiden, M. Petric, R. C. Brunham, and A. J. McGeer. 2003. Identification of severe acute respiratory syndrome in Canada. *N. Engl. J. Med.* 348:1995–2005.
- Riemann, D., A. Kehlen, and J. Langner. 1999. CD13—not just a marker in leukemia typing. *Immunol. Today* 20:83–88.
- Rota, P. A., M. S. Oberste, S. S. Monroe, W. A. Nix, R. Campagnoli, J. P. Icenogle, S. Penaranda, B. Bankamp, K. Maher, M. H. Chen, S. Tong, A. Tamin, L. Lowe, M. Frace, J. L. DeRisi, Q. Chen, D. Wang, D. D. Erdman,

- T. C. Peret, C. Burns, T. G. Ksiazek, P. E. Rollin, A. Sanchez, S. Liffick, B. Holloway, J. Limor, K. McCaustland, M. Olsen-Rasmussen, R. Fouchier, S. Gunther, A. D. Osterhaus, C. Drosten, M. A. Pallansch, L. J. Anderson, and W. J. Bellini. 2003. Characterization of a novel coronavirus associated with severe acute respiratory syndrome. *Science* **300**:1394–1399.
29. Sawicki, D., T. Wang, and S. Sawicki. 2001. The RNA structures engaged in replication and transcription of the A59 strain of mouse hepatitis virus. *J. Gen. Virol.* **82**:385–396.
30. Schickli, J. H., B. D. Zelus, D. E. Wentworth, S. G. Sawicki, and K. V. Holmes. 1997. The murine coronavirus mouse hepatitis virus strain A59 from persistently infected murine cells exhibits an extended host range. *J. Virol.* **71**:9499–9507.
31. Schmidt, I., M. Skinner, and S. Siddell. 1987. Nucleotide sequence of the gene encoding the surface projection glycoprotein of coronavirus MHV-JHM. *J. Gen. Virol.* **68**:47–56.
32. Snijder, E. J., P. J. Bredenbeek, J. C. Dobbe, V. Thiel, J. Ziebuhr, L. L. Poon, Y. Guan, M. Rozanov, W. J. Spaan, and A. E. Gorbalenya. 2003. Unique and conserved features of genome and proteome of SARS-coronavirus, an early split-off from the coronavirus group 2 lineage. *J. Mol. Biol.* **331**:991–1004.
33. Thiel, V., K. A. Ivanov, A. Putics, T. Hertzog, B. Schelle, S. Bayer, B. Weissbrich, E. J. Snijder, H. Rabenau, H. W. Doerr, A. E. Gorbalenya, and J. Ziebuhr. 2003. Mechanisms and enzymes involved in SARS coronavirus genome expression. *J. Gen. Virol.* **84**:2305–2315.
34. Tresnan, D. B., R. Levis, and K. V. Holmes. 1996. Feline aminopeptidase N serves as a receptor for feline, canine, porcine, and human coronaviruses in serogroup I. *J. Virol.* **70**:8669–8674.
35. Wentworth, D. E., and K. V. Holmes. 2001. Molecular determinants of species specificity in the coronavirus receptor aminopeptidase N (CD13): influence of N-linked glycosylation. *J. Virol.* **75**:9741–9752.
36. Williams, R. K., G. S. Jiang, S. W. Snyder, M. F. Frana, and K. V. Holmes. 1990. Purification of the 110-kilodalton glycoprotein receptor for mouse hepatitis virus (MHV)-A59 from mouse liver and identification of a non-functional, homologous protein in MHV-resistant SJL/J mice. *J. Virol.* **64**:3817–3823.
37. Yam, W. C., K. H. Chan, L. L. Poon, Y. Guan, K. Y. Yuen, W. H. Seto, and J. S. Peiris. 2003. Evaluation of reverse transcription-PCR assays for rapid diagnosis of severe acute respiratory syndrome associated with a novel coronavirus. *J. Clin. Microbiol.* **41**:4521–4524.
38. Yeager, C. L., R. A. Ashmun, R. K. Williams, C. B. Cardellicchio, L. H. Shapiro, A. T. Look, and K. V. Holmes. 1992. Human aminopeptidase N is a receptor for human coronavirus 229E. *Nature* **357**:420–422.
39. Zhong, N. S., B. J. Zheng, Y. M. Li, Poon, Z. H. Xie, K. H. Chan, P. H. Li, S. Y. Tan, Q. Chang, J. P. Xie, X. Q. Liu, J. Xu, D. X. Li, K. Y. Yuen, Peiris, and Y. Guan. 2003. Epidemiology and cause of severe acute respiratory syndrome (SARS) in Guangdong, People's Republic of China, in February, 2003. *Lancet* **362**:1353–1358.